Molecular Dynamics of Silver Nanowires Stiffened by Quantum Mechanics

Thomas Prevenslik

***Abstract*—Over the past decade, the observation of significant stiffening of nanowires or NW's has been reported, although some findings suggest there is no stiffening. Because of this uncertainty, research on the mechanism for stiffening has been a subject of great interest. Numerous mechanisms have been proposed that depend on high surface-to-volume ratio of NW's including surface stress and strain – all of which rely on classical physics. However, classical physics in the interpretation of nanoscale behaviour typically leads to unphysical results that are avoided by quantum mechanics. In NW's, quantum mechanics precludes the atoms in NW's from having the heat capacity to conserve the absorption of thermal energy from macroscopic supports by an increase in temperature. Instead, absorbed energy is conserved by frequency up-conversion to the total internal reflection resonance of the NW by quantum electrodynamics, the consequence of which is the production of photons that create charge by the photoelectric effect. Molecular dynamics simulations show the stiffening of NW's is caused by the charge repulsion between atoms creating a state of hydrostatic tension that changes the usual uniaxial stress to a triaxial stress state that by the Poisson effect enhances the Young's modulus consistent with elasticity theory.**

I. Introduction

OVER the past decade, the observation of significant stiffening of NW's has been reported, although some findings suggest there is no stiffening. Because of this uncertainty, research on the mechanism for stiffening has been a subject of great interest. Numerous mechanisms [1] have been proposed including: high surface-to-volume ratio, surface stresses, bulk nonlinear elasticity, surface stiffness, surface tension, surface reconstruction, surface strain and stress, and skin depth energy pinning.

Generally, the stiffening of NW's is not based on direct measurements of material properties, but rather inferred from indirect measurements of increased resistance to buckling, enhanced resonant frequencies, and the like. In contrast, the traditional uniaxial tensile test of a NW gives mechanical properties directly, but is difficult to perform because of the nanoscopic size of the tensile specimen. Nevertheless, Young's modulus and yield stress of fivefold twinned silver NW's was recently [2] measured in tensile tests and found to show stiffening consistent with indirect measurements, the stiffening mechanism thought to be the high surface-to-volume ratio in combination with the annihilation of dislocations at free surfaces and enhanced strain hardening from fivefold twinning. The stiffening mechanisms proposed to date find basis in classical physics [3] contrary to the fact stiffening is not observed at the macroscale, but rather a QM effect only observed in < 100 nm diameter NW's. QM stands for quantum mechanics. Unlike classical physics, only QM having a size effect may explain stiffening of NW's.

In this paper, the QM requirement is invoked that the heat capacity of the atom vanishes at the nanoscale thereby precluding the conservation of thermal energy from macroscopic supports by an increase in temperature, say from the grips in uniaxial tensile tests of NW's. Instead, the absorbed thermal energy is conserved by the creation of photons *inside* the NW by frequency up-conversion to its TIR resonance. QED stands for quantum electrodynamics and TIR for total internal reflection.

Manuscript received September 10, 2012. T. Prevenslik is a retired American with QED Radiations, Discovery Bay, Hong Kong, CHINA. (E-mail: nanoqed@gmail.com and URL: http://www.nanoqed.org).

II. Theory

A. QM Restrictions

Unlike classical physics, QM restricts the heat capacity of nanostructures through the thermal kT energy of the atom thereby precluding conservation of any form of EM energy by an increase in temperature. EM stands for electromagnetic. A comparison of the kT energy of the atom by classical physics and QM by the Einstein-Hopf relation [4] is shown in Fig. 1.

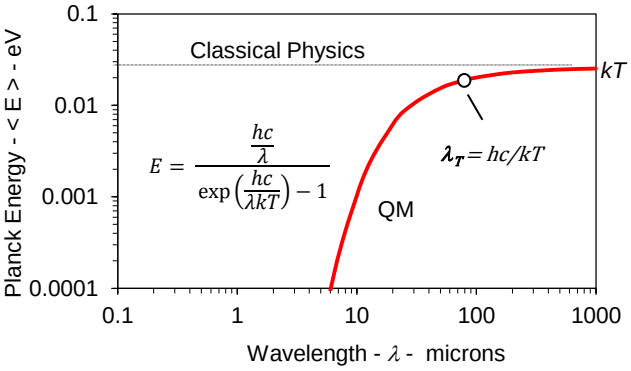

Fig. 1 Heat Capacity of the Atom at 300K
E is Planck energy, h Planck's constant, c speed of light
k Boltzmann's constant, T absolute temperature, and λ wavelength

Classical physics allows the atom to have the same kT energy in submicron nanostructures as in macroscopic bodies. QM differs in that kT energy is only available for $\lambda > \lambda_T$ and otherwise is < kT. At ambient temperature, $\lambda_T \sim 40$ microns. Fig. 1 shows the thermal energy or heat capacity of the atom is < kT for $\lambda < 40$ microns. By QM, atoms under

EM confnement wavelengths $\lambda < 1$ micron have virtually no heat capacity to conserve energy from any EM source by an increase in temperature.

B. TIR Confinement

Lack of heat capacity by QM precludes heat absorbed from EM sources to be conserved in nanostructures by an increase in temperature. The EM energy is proposed conserved by the creation of non-thermal EM radiation by the QED induced frequency up-conversion to the TIR resonance of the nanostructure.

In 1870, Tyndall showed light is trapped by TIR in the surface of a body if the refractive index of the body is greater than that of the surroundings. TIR has an important significance in nanostructures and need not be limited to light absorption. Unlike macroscopic bodies, nanostructures have high surface to volume ratios, and therefore EM energy from any source (lasers, mechanical and Joule heat, electron beam irradiation) is absorbed almost entirely in their surface. Since the nanostructure surface coincides with the TIR wave function, QED induces the absorbed EM energy to undergo spontaneous conversion to surface QED photons However, TIR confinement sustains itself only during EM energy absorption, i.e., absent absorption of EM energy, there is no TIR confinement and QED radiation is not created.

QED relies on complex mathematics as described by Feynman [5] although the underlying physics is simple, i.e., photons of wavelength λ are created by supplying EM energy to a submicron QM box with sides separated by $\lambda/2$. In this way, QED frequency up-converts absorbed EM energy to the TIR resonance described by the characteristic dimension D_C of the nanostructure. The QED photon energy E and frequency υ are:

$$E = h\upsilon, \;\; \upsilon = \frac{c}{\lambda}, \;\; \lambda = 2nD_c \tag{1}$$

where, n is the refractive index of the nanostructure.

C. QED Induced Hydrostatic Tension

In NW's, the prompt conversion of thermal heat from the supports to QED photons at the speed of light is far faster than the phonons at acoustic velocities can respond, thereby essentially negating thermal conduction by phonons. Under TIR confinement across the wire diameter, the QED photons *inside* the wire have Planck energies beyond the ultraviolet (UV). By the photoelectric effect, the QED photons promptly eject electrons to the surroundings leaving positive charge that by electrostatic repulsion produces a stress state of hydrostatic tension.

D. Triaxial Stress State

Unlike the uniaxial stress state in macroscopic tensile specimens, NW's under tension are under a triaxial stress state. Taking the x-y directions in the plane of the wire cross-section and the z direction along its length, the hydrostatic pressure P in terms of stresses σ_x, σ_y, and σ_z,

$$P = \frac{\sigma_x + \sigma_y + \sigma_z}{3} \tag{2}$$

In hydrostatic tension, $\sigma_x = \sigma_y = \sigma_z = P$.

E. QED Induced Pressure

The QED induced pressure P produced in the tensile specimen from thermal kT energy acquired from the grips is obtained by computing the electrostatic repulsion from positive charges produced by the photoelectric effect. However, the pressure P may be upper bound by assuming all the atoms in the NW acquire kT energy at the support temperature T. Provided the QED photon energy $E > 5$ eV, the QM pressure is,

$$P_{QM} = \frac{NkT}{V} = \frac{kT}{\Delta^3} \tag{3}$$

where, N is the number of atoms in the volume V of the NW, i.e., $V/N = \Delta^3$ and Δ is the atomic spacing. . For the silver with $\Delta = 0.409$ nm with grips at $T = 300$ K, $P_{QM} < 6.05 \times 10^7$ Pa ~ 8770 psi.

Other forms of absorbed EM energy also stiffen the NW, e.g., mechanical heat from hysteresis in loading and unloading the tensile specimen.

F. Enhanced Young's Modulus and Yield Strength

In tensile tests of NW's, elasticity theory for the triaxial stress state gives the strain e_z along the wire length,

$$e_z = \frac{1}{Y_o}\left[\sigma_z - \nu\left(\sigma_x + \sigma_y\right)\right] \tag{4}$$

where, ν is Poisson's ratio and Y_O the bulk Young's modulus in the uniaxial stress state.

$$\begin{aligned} \sigma_X' &= \sigma_x + P \\ \sigma_y' &= \sigma_y + P \\ \sigma_z' &= \sigma_z + P \end{aligned} \tag{5}$$

where, σ' includes the pressure stress. Hence, the Young's modulus Y in the triaxial stress state is,

$$Y = \frac{\sigma}{e_z} = \frac{Y_O}{1 - \nu\left(\sigma_X' + \sigma_y'\right)/\sigma_z'}$$

Or,

$$\frac{Y}{Y_O} = \frac{1}{1 - \nu\left(\sigma_x + \sigma_y + 2P\right)/(\sigma_z + P)} \tag{6}$$

For $\sigma_x + \sigma_y < 2P$ and $\sigma_z > P$, the QED enhancement Y/Y_O ratio for Poisson's ratio of silver $\nu = 0.37$ and the incompressible limit is shown in Fig. 2.

Taking the yield of silver $\sigma_z = 6550$ psi and the QM pressure P= 8770 psi, $P / \sigma_z = 1.33$ and $Y/Y_O \sim 63$. But this is only a simplification to describe the basic physics of stiffening in NW's. By the Poisson effect, the σ_x and σ_y stresses reduce the e_z strain from that of the uniaxial stress state, thereby increasing the Young's modulus. Detailed stresses are derived in the molecular dynamics (MD) simulations. Regardless, the enhancement of Young's modulus is significant. The silver yield strength is enhanced the same as that for Young's modulus.

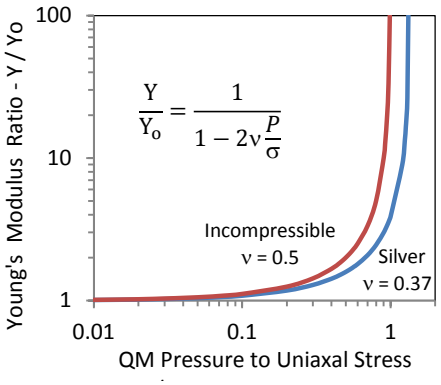

Fig. 2 QED Enhancement of Young's Modulus

III. Simulation

Standard MD computer programs based on statistical mechanics that implicitly assume the atoms have heat capacity could not be used to derive the Young's modulus of silver NW's. Because of this, the Leapfrog algorithm [6] was modified to accommodate the QM restrictions that require the atom's heat capacity to vanish.

A. NW Model

The NW model geometry selected was a square cross\-section having sides w and length L as illustrated in the VMD graphics in Fig. 3. The silver wire was modeled in the FCC configuration with an atomic spacing of 4.09 A comprising 550 atoms having sides w = 8.18 A and length L = 87.9 A.

Fig. 3 MD Model of NW under Longitudinal Loading

B. Lennard-Jones Potential

The L-J potential [7] was used to simulate the atomic potential U of the silver NW.

$$U_{ij} = 4\varepsilon\left[\left(\frac{\sigma}{R_{ij}}\right)^{12} - \left(\frac{\sigma}{R_{ij}}\right)^{6}\right] \qquad (7)$$

where, R_{ij} the interatomic spacing and for silver σ = 2.644 A and ε = 0.345 eV.

C. Electrostatic Repulsion

The QM pressure is caused by the electrostatic repulsion of atoms from charges created by the QED induced photoelectric effect. The electrostatic potential U_{ES}, for the atom as a sphere of radius R_{atom} having electron charge e,

$$U_{ES} = \frac{3e^2}{20\pi\varepsilon_o R_{atom}} \qquad (8)$$

where, ε_o is the permittivity of the vacuum.

D. Thermal kT Energy

In the NW, the thermal kT energy U_{kT} of the atom depends on the temperature $T_{grip\ of}$ the grips,

$$U_{kT} = \frac{3}{2}kT_{grip} \qquad (8)$$

E. Stress Calculation

The MD response gives pressure within the specimen and not the stresses. In the controversy [8] as to whether the virial stress gives the Cauchy stress, the virial stress in terms of the dimensionality n of the constraints is::

$$\sigma_{ij}^{y} = \frac{1}{V}\sum_{\alpha}\left[\sum_{\beta=1}^{N}\left(R_i^{\alpha} - R_i^{\beta}\right)F_j^{\alpha\beta} - nkT\right] \qquad (9)$$

where, β takes values 1 to N neighbors of atom α, R_i^{β} is the position of atom β along direction i, $F_j^{\alpha\beta}$ is the force (along direction j) on atom α due to atom β, and *V* is the volume.

However, the controversy over virial and Cauchy stress may be irrelevant at the nanoscale as by QM the thermal kT energy of the atom vanishes. Hence, the virial stress σ_{xx} is,

$$\sigma_x^{y} = \frac{1}{V}\sum_{\alpha}\sum_{\beta=1}^{N}\left(R_x^{\alpha} - R_x^{\beta}\right)F_x^{\alpha\beta} \qquad (10)$$

with the σ_y and σ_z stress is similarly defined.

F. MD Pressure

The MD pressure P within the NW model [6] during equilibration and loading is,

$$P = P_{QM} + \left(NkT + \frac{1}{3}\sum_{\alpha}\sum_{\alpha>\beta} r\frac{dU}{dr}\right)/V \qquad (11)$$

G. Equilibration and Loading

1. Equilibration During equilibration, the NW was fixed at the left end and free at the right end. At the fixed end, only the z-coordinates of the atoms on were fixed; the x and y atom positions were free to move. With the atoms in the plane of the left end corresponding to the origin of the xyz system, the free end is located at z = L

Consistent with the QM requirement that the atoms have vanishing heat capacity, the absolute temperature was held at < 0.1 K by the Nose-Hoover thermostat. During equilibration, the QM pressure P_{QM} is not used.

2. Loading The NW was displacement loaded by a step change δ in the z-direction at z = L. The force $F = AY_O\,\delta / L$ where the axial stress σ = F/A and strain ε = δ / L.

The QM pressure P_{QM} tending to separate the atoms is simulated by defining the fraction η of the electrostatic U_{ES} energy corresponding to the thermal kT energy of the atom.

$$\eta = \frac{U_{kT}}{U_{ES}} = \frac{10\pi\varepsilon_o k R_{atom} T_{grip}}{e^2} \qquad (12)$$

Taking T_{grip} = 300 K for the silver atom having R_{atom} = 1.45 A, e = $1.6\text{x}10^{-19}$ C, the fraction η = 0.0065. During the MD solution, the Nose-Hoover thermostat maintained the temperature T < 0.01 K.

H. Response

The MD response was obtained for uniaxial and triaxial stress states at time steps from 1-5 fs.

1. Uniaxial In the uniaxial response, the QM pressure induced electrostatic repulsion was excluded. Equilibration for 5000 steps was followed by displacement loading to 10000 steps. For δ = 0.5 A, the displacement loading is shown in Fig. 4.

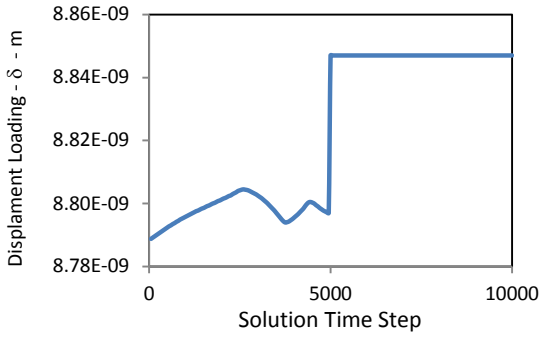

Fig. 4 Displacement Loading

Before the displacement load, the σ_x, σ_y, and σ_z stresses < 100 psi. Upon displacement δ loading, the stresses increased and at convergence, the σ_x and σ_y stresses vanished leaving only the σ_z stress. The σ_x and σ_y stresses were identical as shown for δ = 0.5 A in Fig. 5.

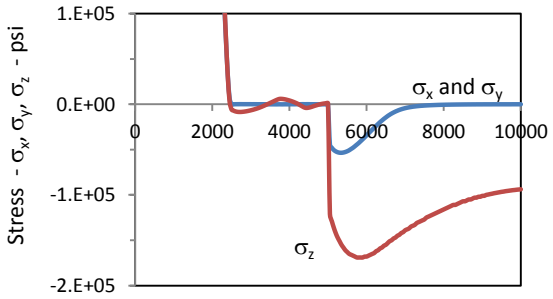

Fig. 5 Uniaxial Stress State

Upon convergence at 10000 steps, the displacement loading δ = 0.15, 0.25, and 0.5 A was found to be approximately linear giving Young's moduli $Y_o \sim 16x10^6$ psi as shown in Fig. 6.

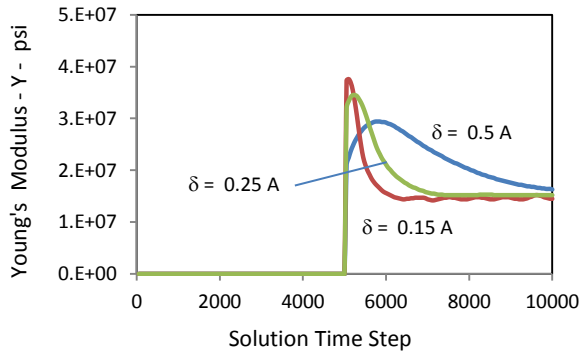

Fig. 6 Uniaxial Young's Modulus

2. Triaxial The triaxial response included the QM pressure through the electrostatic repulsion. For full kT energy corresponding to η = 0.0065, the MD solution for displacement δ = 0.5 A consisted of equilibration for 5000 steps followed by loading for an additional 5000 steps as shown in Fig. 7. Unlike uniaxial stress, the σ_x and σ_y stresses did not vanish after equilibration and loading. It is of note, that attempts to use a constant QM pressure alone instead of electrostatic repulsion failed as the σ_x and σ_y stresses vanished as for the uniaxial stress state.

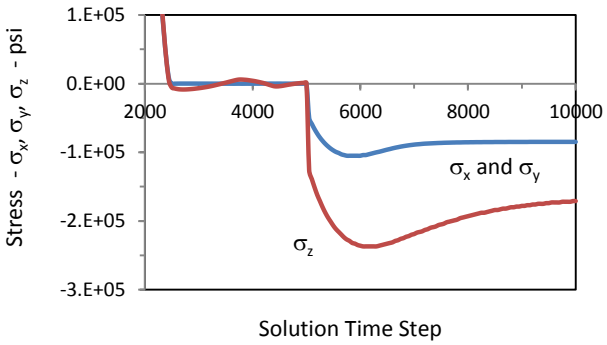

Fig. 7 Triaxial Stress State - Stresses

The Young's modulus Y and Poisson's ratio ν for displacement loading δ = 0.5 A at fractions η = 0.0065, 0.003 and 0.001 are shown in Fig. 8 and 9.

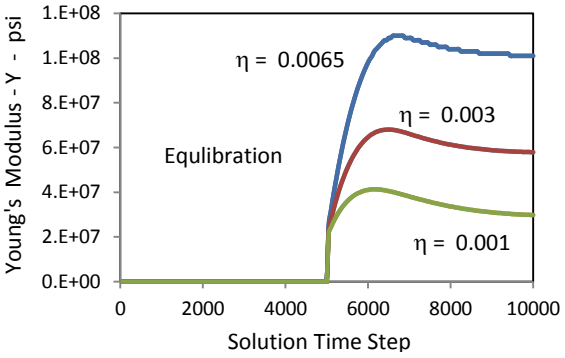

Fig. 8 Triaxial Stress State – Young's Modulus

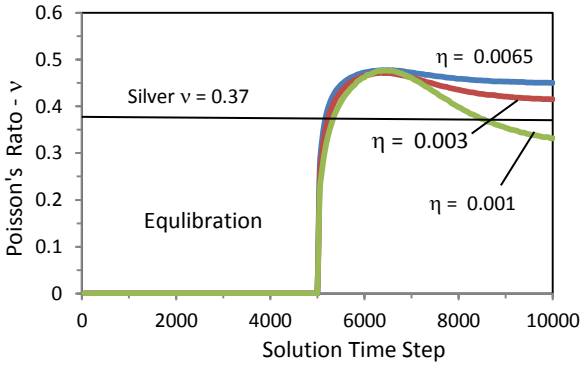

Fig. 9 Triaxial Stress State – Poisson's Ratio

IV. DISCUSSION

A. MD Solution and Comparison to Data

Simulating the QM pressure with the fraction η of the kT energy by electrostatic repulsion produces the solutions shown in Fig. 8. After convergence at 10000 steps, full kT energy corresponding to η = 0.0065 gives Young's modulus Y = $100x10^6$ psi; while η = 0.003 and 0.001 give Y = 60 and $30x10^6$ psi, respectively. The correct Young's modulus is determined from the Poisson/s ratio of silver ν = 0.37. Interpolation gives the η = 0.002 solution is close to that for silver as shown in Fig. 9. Hence, the Young's modulus of the NW is about $45x10^6$ psi. With the uniaxial Young's modulus Yo ~ 16 x 10^6 psi, the stiffening enhancement is Y/Yo ~ 3. The MD solution for η = 0.002 of silver NW's means only 2/6.5 or about 30 % of the full kT energy stiffens the NW, the remaining kT energy lost to the surroundings as QED radiation.

Experimental data (Table I of [2]) on 34 nm diameter silver NW's show Young's moduli of Y = $26x10^6$ psi. In contrast, the MD solution for the smaller 8 A square silver NW gave Y = $45x10^6$ psi, although the MD solution appears reasonable at about 2x that for the 34 nm NW.

B. EM Energy Sources and Stiffening

Only the kT energy of the grips was considered as the heat source, but any EM energy absorbed by the NW also produces the stiffening effect. In this regard, the strain hardening (Fig. 2(a) of [2]) under a sequence of loading and unloading to raise the ultimate tensile strength (UTS) to about 300,000 psi, or about 45x that of the yield of bulk silver at 6550 psi. The strain hardening is explained by dislocation-induced shear, but the dislocations produce mechanical heat that like the thermal kT energy of the grips cannot be conserved by an increase in temperature. Instead, it is more likely conservation of dislocation induced mechanical heating proceeds by QED induced triaxial stress states that enhance the UTS by strain hardening as depicted for the Young's modulus Y in Fig. 2.

Passing current through NM's is a source of Joule heat that again is induced by QED to enhance the Young's modulus. Indeed, electron beam irradiation is shown [9] to enhance the Young's modulus of tin oxide NW's by 40%.

C. Shape of Fracture Surface

In the tensile tests of silver NW, the fracture surface is unusual. Unlike macroscopic tensile specimens, the NW specimen showed no diameter reduction or necking prior to failure as shown in Fig. 10.

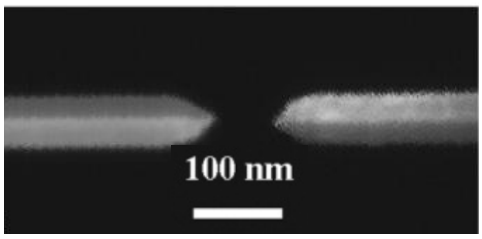

Fig. 10 Fracture Surface of Silver Nanowire

Dislocation-induced shear is thought [2] to explain the localized fracture surface. However, it is more likely the shape fracture surface is caused by the removal of silver atoms by Coulomb explosion from QED induced charge repulsion during strain hardening. Verification of Coulomb explosion of NW's by searching the SEM chamber for silver atoms or monitoring their emission during tensile testing is suggested. MD simulations of Coulomb explosions in NW's under tensile testing are planned.

V, CONCLUSIONS

Classical physics assumes the atom always has heat capacity. QM differs by restricting the atom's heat capacity to vanishing small levels in nanostructures. Conserving absorbed EM energy by the QED induced creation of photons in the nanostructure surface avoids unphysical findings and heat transfer anomalies.

In tensile tests of silver NW's, the QED photons are created by EM energy from the temperature of the grips that hold the NW in combination with the heat associated with strain hardening. The QED photons charge the silver atoms by the photoelectric effect to induce electrostatic repulsion placing the NW under high hydrostatic tension. The Young's modulus of NW's is enhanced above bulk because the hydrostatic tension pressure reduces the longitudinal strain by the Poisson effect of classical elasticity.

MD solutions of 8 A square NW show the QED induced charge repulsion of silver atoms give Young's moduli of $45x10^6$ psi comparable to data of for the 34 nm NW. MD solutions are computationally intensive and require computing power beyond the PC, especially for the larger 34 nm diameter NW's.

The QED induced stiffening of NW's in tensile tests occurs anytime EM energy is absorbed including thermal energy from grips, mechanical heat from repeated loading and unloading, and electron beam irradiation.

REFERENCES

[1] X. J. Lu, J. W. Li, Z. F. Zhou, L. W. Yang, Z. S. Ma, G. F. Xie, Y. Pan, and C. Q. Sun, "Size-induced elastic stiffening of ZnO nanostructures: Skin-depth energy pinning," *App. Phys. Lett.*, vol. 94, 131902, 2009.

[2] Y. Zhu, Q. Qin, F. Xu, F. Fan, Y. Ding, T. Zhang, B. J. Wiley, and Z. L. Wang., "Size effects on elasticity, yielding, and fracture of silver nanowires: In situ experiments," *Phys. Rev. B*, 85, 045443, 2012.

[3] C. Kittel, *Introduction to Solid State Physics*, 7th ed. Wiley, New York. 1996.

[4] A. Einstein and L. Hopf, "Statistische Untersuchung der Bewegung eines Resonators in einem Strahlungsfeld," *Ann. Physik*, vol. 33, pp. 1105-1120, 1910.

[5] R. Feynman, *QED: The Strange Theory of Light and Matter*. Princeton University Press, 1985.

[6] M. P. Allen and D. J. Tildesley, *Computer Simulations of Liquids*, (Oxford: Clarendon Press: 1987).

[7] P. Guan, D. R. Mckenzie and B. A. Pailthorpe, "MD simulations of Ag film growth using the Lennard-Jones potential,", *J. Phys.: Condens. Matter 8,* pp. 8753–8762, 1996.

[8] A. K. Subramaniyan and C. T. Sun, "Continuum Interpretation of Virial Stress in Molecular Simulations," *Int. J. of Solids and Structures*, vol. 3, pp. 16, 2008.

[9] J. Zang, L. Bao, R. A. Webb, and X, Li, "Electron Beam Irradiation Stiffens Zinc Tin Oxide Nanowires," *Nano Lett.*, vol. 11, pp. 4885–4889, 2011.